Journal of Agricultural Science; Vol. 7, No. 4; 2015
ISSN 1916-9752 E-ISSN 1916-9760
Published by Canadian Center of Science and Education

Suppression of Hepatitis B Virus Production and Inflammatory Response *in vitro* and *in vivo* by *Mormodica charantia* Compound EMCDO

Chi-I Chang[1], Chiy-Rong Chen[2], Yo-Chia Chen[1], Kuei-Wen Cheng[1], Bo-Wei Lin[1], Yun-Wen Liao[1] & Wen-Ling Shih[1]

[1] Department of Biological Science and Technology, National Pingtung University of Science and Technology, Pingtung, Taiwan

[2] Department of Life Science, National Taitung University, Taitung, Taiwan

Correspondence: Department of Biological Science and Technology, National Pingtung University of Science and Technology, 1, Shuefu Rd., Neipu, Pingtung, 91201, Taiwan. Tel: 886-8-770-3202 ext. 5192. E-mail: wlshih@mail.npust.edu.tw

Received: January 8, 2015 Accepted: February 8, 2015 Online Published: March 15, 2015

doi:10.5539/jas.v7n4p112 URL: http://dx.doi.org/10.5539/jas.v7n4p112

Abstract

Eight compounds were purified from *Mormodica charanti*, and their chemical structures were determined in this study. Their anti-HBV and anti-inflammation activities were investigated. Compound EMCDO exhibited the most efficient effect in terms of reducing HBV surface antigen, e antigen and viral DNA levels in HBV particles or surface antigen-producing cells 2.2.15 and PLC/PRF/5, respectively. Tumor suppressor p53 played a significant role in EMCDO-mediated anti-HBV effects. Pretreatment with EMCDO prevented 2.2.15 cells-induced tumor formation in a nude mice subcutaneous model. The anti-HBV and anti-tumor activities of EMCDO were better than those of oltipraz, an inhibitor of HBV transcription. EMCDO reduced the proinflammatory cytokines and mediators in LPS-treated RAW264.7 cells in a dose-dependent manner. The LPS-upregulated phosphorylation level of Iκα was reduced in the presence of EMCDO. The transcription activity of NF-κB was increased in cells treated with EMCDO. Utilization of a mouse ear edema model further confirmed the activity of EMCDO against TPA-elicited inflammation.

Keywords: *Mormodica charantia,* HBV, nude mice, RAW264.7, inflammation

1. Introduction

Hepatitis B virus (HBV) is the major cause of acute and chronic hepatitis and a serious liver disease (Maddrey, 2000). Although HBV has been vaccine-preventable since 1981, the infection rates have not declined over the past several years, leading to the conclusion that we have allowed gaps in screening, prevention, and treatment to go unchecked (Chemin, 2010). Hepatocellular carcinoma therefore remains a significant problem, owing to the high mortality rate and difficulty in treatment using existing medical drugs and approaches. In view of the limited treatment options and grave prognosis, preventive control is considered the best strategy to lower the current morbidity and mortality associated with liver-related disease (Elgouhari, Abu-Rajab Tamimi, & Carey, 2008). A close connection between inflammation and cancer has been long suspected. It is well-known that inflammation increases the risk and accelerates the development of various types of cancer. A clear example of inflammation-related cancer is hepatocellular carcinoma (HCC) (Berasain et al., 2009a). Thus, HBV chronic infection and hepatitis are two risk factors for hepato-carcinogenesis, suggesting that the strategy for the prevention of liver carcinogenesis should consist of anti-HBV and anti-inflammation approaches, which could reduce the further development of liver cirrhosis and carcinoma (Berasain et al., 2009b).

There is a growing body of *in vitro* evidence demonstrating the inhibitory effects of certain natural products on liver cancer cells *via* various regulatory mechanisms (Aslam et al., 2012). Triterpenes have previously been purified from the bitter melon, and detailed analysis has shown that the compounds consist in the main of cucurbitane-type triterpenoids (Liao et al., 2012). The anti-carcinogenic activity of cucurbitane-type triterpenoids has been clearly demonstrated in two-stage carcinogenesis testing in skin tumors induced by peroxynitrite ($ONOO^-$) as an initiator and TPA as a promoter in a specific pathogen-free mouse model (Takasaki et al., 2003).

Additionally, the inhibitory effects of mogroside V and 11-oxo-morgroside V on Epstein-Barr virus early antigen (EBV-EA) activation by TPA in Raji cells have been confirmed (Akihisa et al., 2007), and an anti-HIV inhibitory activity of some cucurbitane-type triterpenoids isolated from the tubers of *Hemsleya endecaphylla* has also been observed (Chen et al., 2008).

Inflammation is a critical and complex immune event. An aberrant or intensified inflammatory response has been described for numerous diseases, including cancer progression (Marusawa & Jenkins, 2014). Several triterpenoids from various plants, such as lupeol, a triterpenoid isolated from Lonchocarpus araripensis Benth., reduce the production of mucus and overall inflammation in the lung (Vasconcelos et al., 2008); the triterpenoid acetyl-11-keto-β-boswellic acid (AKβBA) isolated from the oleogum resin of *Boswellia carterii* functioned as a NF-κB inhibitor and alleviated skin inflammation in a psoriasis mouse model (Wang et al., 2009).

Although many bioactive beneficial compounds have not yet been well-defined, there exists scientific evidence suggesting potential anti-virus, immune modulation and cancer prevention effects. The aim of this study was to evaluate the potential against HBV and acute inflammation of compound EMCDO isolated from *Mormodica charantia*, as well as elucidate the host factors and mechanisms involved. Taken together, the findings of this project will enable us to improve knowledge and understanding of the anti-HBV, anti-inflammation and chemoprevention effects and mechanisms of some potential natural products, and it is hoped that the outcome will also be of use in assisting the development of biological agents for the prevention of HBV replication and further reducing the incidence of liver cancer.

2. Method

2.1 Cell Culture

2.2.15 cells secrete HBV surface antigen (HBsAg), e antigen (HBeAg), nucleocapsids and virions (Acs et al., 1987). The hepatoma cell line PLC/PRF/5 possesses HBV DNA sequence integration at several sites and produces HBsAg into growth medium. RAW264.7 is a mouse leukemic monocyte macrophage cell line used for an anti-inflammation cell-based system. Three cell lines were cultured in DMEM supplemented with 10% FBS containing 100 U/mL of penicillin and 100 μg/mL of streptomycin at 37 °C in a 5% CO2 humidified incubator.

2.2 Mormodica Charantia Compounds

Fruit of *M. charantia* were purchased from contracted farmers in Kaohsiung, Taiwan. The plant material was identified by Prof. Sheng-Zehn Yang, Curator of the Herbarium, National Pingtung University of Science and Technology. A voucher specimen was deposited in the laboratory of Dr. Chi-I Chang (Pingtung, Taiwan). Dried fruit (30 kg) of *M. charantia* L. wild variant WB24 was mechanically powdered and extracted five times with methanol (60 L) at room temperature (7 days each). The combined MeOH extract was then evaporated under reduced pressure to afford a black residue, which was suspended in H_2O (4 l) and partitioned sequentially using ethyl acetate (EA) and *n*-butanol (*n*-BuOH) (5 × 4 l). The *n*-BuOH fraction (966 g) was chromatographed on a Diaion HP-20 column (150 × 10 cm) and eluted using mixtures of water and methanol of reducing polarity as eluents to yield twenty-five fractions: fr. 1 [9000 ml, water], fr. 2 [6000 ml, water–methanol (98:2)], fr. 3 [6000 ml, water–methanol (95:5)], fr. 4 [6000 ml, water–methanol (93:7)], fr. 5 [6000 ml, water–methanol (90:10)], fr. 6 [6000 ml, water–methanol (88:12)], fr. 7 [6000 ml, water–methanol (85:15)], fr. 8 [6000 ml, water–methanol (83:17)], fr. 9 [6000 ml, water–methanol (80:20)], fr. 10 [(7000 ml, water–methanol (75:25)], fr. 11 [7000 ml, water–methanol (70:30)], fr. 12 [7000 ml, water–methanol (65:35)], fr. 13 [7000 ml, water–methanol (60:40)], fr. 14 [7000 ml, water–methanol (55:45)], fr. 15 [7000 ml, water–methanol (50:50)], fr. 16 [1000 ml, water–methanol (45:55)], fr. 17 [7000 ml, water–methanol (40:60)], fr. 18 [7000 ml, water–methanol (35:65)], fr. 19 [7000 ml, water–methanol (30:70)], fr. 20 [(7000 ml, water–methanol (25:75)], fr. 21 [7000 ml, water–methanol (20:80)], fr. 22 [7000 ml, water–methanol (15:85)], fr. 23 [7000 ml, water–methanol (10:90)], fr. 24 [7000 ml, water–methanol (5:95)], and fr. 25 (10000 ml, methanol). Fraction 16 (6.1 g) was further subjected to Sephadex LH-20 column chromatography (5 × 50 cm) with gradient elution (water–methanol,1:1 to 0:1) to afford six fractions (800 ml each), frs 16A–16F. Fr. 16B (0.8 g) was subjected to column chromatography over Si gel with elution by CH_2Cl_2–MeOH (1:0 to 9:1) and semipreparative HPLC with elution by CH_2Cl_2–EA (10:1) to yield compound RA2-117 (95 mg). Fr. 16C (4.2 g) was subjected to column chromatography over Si gel with elution by CH_2Cl_2–MeOH (1:0 to 6:1) and semipreparative HPLC with elution by hexane–acetone (6.5:3.5) to yield compounds RA2-8 (21 mg), RA2-20 (27 mg), RA2-52 (12 mg), and CH93 (16 mg). Fr. 16D (2.2 g) was subjected to column chromatography over Si gel with elution by CH_2Cl_2–MeOH (1:0 to 4:1) and semipreparative HPLC with elution by hexane–EA (7:3) to yield compounds EMCDO (87 mg), RA2-11 (206 mg), and RA2-289 (15 mg).

2.3 Reagents, Kits and Plasmids

Oltipraz, an efficient anti-HBV compound (Chi et al., 1998), was purchased from Sigma. Lipopolysaccharide (LPS) is a well-known inflammation inducer on RWA264.7 cells, and the anti-inflammation compound curcumin could be served as positive control in this cell system. LPS, curcumin, as well as trypan blue were also purchased from Sigma. Dominant negative p53 (p53DN) was purchased from Clontech, which expressed mutated p53 protein by a G to A conversion at nucleotide 1017. HBsAg and HBeAg ELISA kits were purchased from General Biological Corporation (Taipei, Taiwan). An α-fetoprotein (AFP) testing ELISA kit was obtained from Panomics. Three cytokines ELISA kits were purchased from BD Biosciences. All antibodies were purchased from Cell Signaling Tecnology.

2.4 Semi-Quantitative Polymerase Chain Reaction

The primer design was derived from HBV S gene: forward primer 5′-CACATCAGGATTCCTAGGACC-3′(nt 166 to 186); reverse primer 5′-GGTGAGTGATTGGAGGTTG-3′(nt 339 to 321) (Abe et al., 1999). 2.2.15 cells were treated with different concentrations of EMCDO or oltipraz for 3 days, and the HBV particles in conditioned medium were harvested and subjected to HBV DNA isolation using a viral DNA purification kit (Invitrogen). PCR cycles consisted of 3 min initial denaturation at 95 °C, then 30s denaturation at 94 °C, 45s annealing at 55 °C and 90s extension at 72 °C. The linearity of the PCR reactions was checked at different cycle numbers. The plateau phase became apparent after 32 cycles; thus, after a serial check of PCR product, we selected 28 cycles to analyze the HBV DNA level in our system (Netea et al., 1996). The 173bps PCR product was analyzed by electrophoresis on 2% agarose gels stained with ethidium bromide. The EC50s of the compounds were calculated according to the literature (Alexander, Browse, Reading, & Benjamin, 1999).

2.5 Western Blotting and Luciferase Assay

Western blotting analysis was performed as described in our previous studies (Chang et al., 2013; Shih et al., 2013). p53-luc plasmid expressed the firefly luciferase gene is controlled by a synthetic promoter that contains direct repeats of the transcription recognition sequences for the p53 (Stratagene). NF-κB-luciferase was also obtained from Stratagene. Cells were seeded and transfected with luciferase reporter plasmid together with pRKβGAL plasmid using Lipofectamine reagent (Invitrogen). Luciferase activity was determined using a Luciferase Assay System (Promega) and normalized for transfection efficiency by measuring the β-galactosidase activity using a β-Galactosidase Enzyme Assay System (Promega).

2.6 IC_{10} and IC_{50} Determination

Cells were attached onto a 96-well plate then exposed to serial dilutions of compound (1-50 μg/ml) for various durations of incubation. Medium containing the compound was changed every 2 days. The cell viability was measured by MTT assay (Stockert, Blazquez-Castro, Canete, Horobin, & Villanueva, 2012), and the cytotoxic response of RAW264.7 was evaluated by trypan blue exclusion (Shih, Kuo, Chuang, Cheng, & Doong, 2000). The 50% and 10% inhibitory concentrations of the compound were calculated using the formula: $\%IC = [1-(A_{570test}/A_{570cont})] \times 100$, where % IC = % inhibition of cell proliferation, $A_{570test}$ = absorbance of test sample, $A_{570cont}$ = absorbance of control sample (Cetin & Bullerman, 2005).

2.7 Toxicity in Mice

Two groups of both sexes mice were formed, each containing 6 mice. The first group was used as the control group, which received corn oil solvent, while the second group of mice was administered 500 mg/kg body weight of EMCDO via the intraperitoneal route. During 14 days observation, the general behavior was recorded every day. At the end of the experiment, all mice were sacrificed, the organs examined, and blood collected and subjected to biochemical analysis. During the period, the behaviors displayed, such as nervous excitation, depression, reflexes, muscular and activities weakness, salivation, food ingestion and diarrhea, were recorded. All collected organs were weighed and subjected to histopathological investigation by two independent pathologists. On the 15th day, serum was collected and the biochemical markers of liver and renal function were studied. Liver and renal functions were evaluated by determination of glutamic oxaloacetic transaminase (GOT), glutamic pyruvic transaminase (GPT), creatinine and blood urea nitrogen (BUN) (Wu et al., 2011).

2.8 Tumor Prevention in a Mouse Model

18 6-week-old nude mice were purchased from BioLASCO (Taiwan). The mice were divided into 3 groups randomly, one negative control group treated with corn oil, one group treated with 50 mg/kg EMCDO, and the final group treated with 50 mg/kg oltipraz. The sample was injected every day *via* the intraperitoneal route for 7 days, then 1×10^6 2.2.15 cells in100μl medium were inoculated *via* the subcutaneous route. Mice were injected with sample every 2 days for 8 weeks, and the tumor size was measured. The general behavior was also recorded.

At the 56th day after 2.2.15 cell inoculation, blood was collected and serum was isolated, then subjected to liver and renal function evaluation.

2.9 TPA-Induced Ear Edema Mouse Model

8-week-old Balb/c mice were divided into 5 groups, each containing 5 mice. Edema was induced by topical application of 2 μg/20 μl acetone to the inner and outer ear surfaces of each ear. Thirty minutes later, the inner and outer surfaces of both ears were treated with 20 μl of the tested compounds, including acetone vehicle, anti-inflammation drug indomethacin 1.25 μg/20 μl acetone per ear and EMCDO at three different concentrations. The ear thickness was measured using a pocket thickness gauge before and 30 mins after inflammation induction, followed by compound treatment. The ear thickness was then measured at various time points. The anti-inflammation ability was expressed as a edema inhibition percentage: % inhibition = (Tc-Tt)/Tc, where Tc and Tt respectively represented the average thickness with vehicle and compound treatment.

2.10 Statistical Analysis

Data were analyzed by Student's *t*-test; the data are presented as the mean ± standard deviation (SD). $P < 0.05$ was taken to indicate significant differences.

3. Results

3.1 Chemical Structure, Physical and Spectral Data (IR, MS, and NMR) of the Eight Tested Compounds

Eight cucurbitane-type triterpenes, 5*β*,19-epoxy-19(*R*)-methoxycucurbita-6,23(*E*),25-triene-3*β*-ol (RA2-8), 5*β*,19-epoxy-25-methoxycucurbita-6,23(*E*)-dien-3*β*-ol (EMCDO), (23*E*)-7*β*,25-dimethoxycucurbita-6,23(*E*)-dien-3*β*-ol (RA2-11), 5β,19-epoxy-19(*S*)-methoxycucurbita-6,23(*E*)-diene-3*β*,25-diol (RA2-20), (23*E*)-3*β*-hydroxy-7*β*,25-dimethoxycucbita-5,23-dien-19-al (RA2-52), 5β,19-epoxy-19(*S*),25-dimethoxycucurbita-6,23(*E*)-diene-3*β*-diol (RA2-117), (23*E*)-7*β*-methoxycucurbita-6,23(*E*)-diene-3*β*,25-diol (RA2-289), and (23*E*)-3*β*,7*β*,25-trihydroxycucbita-5,23-dien-19-al (CH93), were isolated from the *n*-BuOH soluble fraction of the methanol extract of *M. charantia* fruit (Figure 1). The chemical structures of these compounds were identified by comparing their physical and spectral data (IR, MS, and NMR) with the values described in the literature. The IR, MS, and NMR data of RA2-10, RA2-11, RA2-117, and RA2-289 were reported in our previous study (Chang et al. 2008).Here, we only describe the physical and spectral data of the remaining four compounds, RA2-8, RA2-20, RA2-52 and CH93.5*β*,19-epoxy-19(*R*)-methoxycucurbita-6,23(*E*),25-trien-3*β*-ol (RA2-8) Amorphous white powder; ^{1}H NMR (400 MHz, $CDC1_3$) δ: 0.83 (3H, s, H-30), 0.85 (3H, s, H-18), 0.87 (1H, d, *J* = 6.4 Hz, H-21), 0.92 (3H, s, H-28), 1.20 (3H, s, H-29), 1.81 (3H, s, H-26), 3.41 (1H, brd, *J* = 6.9 Hz, H-3), 3.42 (3H, s, 19-OCH_3), 3.94 (1H, brd, *J* = 9.6 Hz, 3-OH), 4.63 (1H, s, H-19), 4.84 (2H, brs, H-27), 5.60 (1H, brd, *J* = 15.6 Hz, H-23), 5.60 (1H, dd, *J* = 3.2, 10.0 Hz, H-7), 5.97 (1H, dd, *J* = 2.4, 10.0 Hz, H-6), 6.10 (1H, d, *J* = 15.6 Hz, H-24); ^{13}C NMR (100 MHz, $CDCl_3$) δ: 14.7 (C-18), 17.4 (C-1), 18.7 (C-26), 18.7 (C-21), 19.8 (C-30), 20.5 (C-29), 23.2 (C-11), 24.1 (C-28), 27.2 (C-2), 28.0 (C-16), 30.5 (C-12), 33.5 (C-15), 36.6 (C-20), 37.3 (C-4), 39.8 (C-22), 40.5 (C-10), 41.6 (C-8), 45.1 (C-13), 48.0 (C-9), 48.3 (C-14), 50.3 (C-17), 58.3 (19-OCH_3), 76.2 (C-3), 86.7(C-5), 112.1 (C-19), 114.1 (C-27), 129.4 (C-23), 131.0 (C-6), 132.8 (C-7), 134.1 (C-24), 142.2 (C-25); EI-MS (70 eV) *m/z* (rel. int.): 450 $[M-H_2O]^+$ (10), 408 (82), 389 (30), 309 (55), 173 (90), 157 (50), 109 (82), 81 (100). 5*β*,19-epoxy-19(*S*)-methoxycucurbita-6,23(*E*)-diene-3*β*,25-diol (RA2-20) Amorphous white powder, ^{1}H NMR (400 MHz, $CDC1_3$) δ: 0.82 (3H, s, H-30), 0.85 (3H×2, s, H-18, H-28), 0.86 (3H, d, *J* = 5.4 Hz, H-21), 1.21 (3H, s, H-29), 1.27 (3H×2, s, H-26, 27), 2.22 (1H, brs, H-8), 2.26 (1H, m, H-10), 3.37 (3H, s, 19-OCH_3), 3.40 (1H, brs, H-3), 3.70 (1H, d, *J* = 10.4 Hz, 3-OH), 4.40 (1H, s, H-19), 5.49 (1H, dd, *J* = 3.2, 10.0 Hz, H-7), 5.56 (2H, m, H-23, 24), 6.07 (1H, dd, *J* = 2.0, 10.0 Hz, H-6); ^{13}C NMR (100 MHz, $CDCl_3$) δ: 15.0 (C-18), 16.5 (C-1), 18.6 (C-21), 19.9 (C-30), 20.6 (C-29), 21.4 (C-2), 24.4 (C-28), 27.1 (C-11), 27.8 (C-16), 29.8 (C-26), 29.9 (C-27), 30.3 (C-12), 33.4 (C-15), 36.2 (C-20), 37.0 (C-4), 37.8 (C-10), 39.0 (C-22), 45.1 (C-13), 48.0 (C-14), 48.9 (C-9), 49.7 (C-8), 50.1 (C-17), 57.3 (19-OCH_3), 70.6 (C-25), 76.1 (C-3), 85.0 (C-5), 114.7 (C-19), 125.2 (C-23), 130.5 (C-7), 133.0 (C-6), 139.5 (C-24); EI-MS (70 eV) *m/z* (rel. int.): 426 $[M-HCO_2CH_3]^+$ (10), 408 (14), 309 (15), 281 (9), 239 (11), 187 (21), 172 (39), 157 (31), 109 (50), 91 (100), 84 (100), 69 (59), 55 (78). 3*β*-hydroxy-7*β*,25-dimethoxycucurbita-5,23(*E*)-dien-19-al (RA2-52) Amorphous white powder; ^{1}H NMR (400 MHz, $CDC1_3$) δ: 0.71(3H, s, H-30), 0.87 (1H, d, *J* = 6.8 Hz, H-21), 0.88 (3H, s, H-18), 1.02 (3H, s, H-28), 1.20 (3H×2, s, H-26, 27), 1.21 (3H, s, H-29), 3.09 (1H, s, 25-OCH_3), 3.16 (1H, brs, H-7), 3.20 (1H, s, 7-OCH_3), 3.41 (1H, brd, *J* = 6.4 Hz, 3-OH), 3.56 (1H, brs, H-3), 5.34 (1H, d, *J* = 15.6 Hz, H-24), 5.48 (1H, ddd, *J* = 5.6, 8.4, 15.6 Hz, H-23), 5.90 (1H, d, *J* = 8.4 Hz, H-6), 9.70 (1H, s, H-19); ^{13}C NMR (100 MHz, $CDCl_3$) δ: 14.8 (C-18), 18.0 (C-30), 18.7 (C-21), 20.7 (C-1), 22.2 (C-11), 25.2 (C-29), 25.7 (C-27), 26.0 (C-26), 26.9 (C-28), 27.3 (C-16), 28.3 (C-2), 28.8 (C-12), 34.7 (C-15), 35.9 (C-10), 36.0 (C-20), 39.2 (C-22), 41.4 (C-4), 44.4 (C-8), 45.5 (C-13), 47.3 (C-14), 49.8 (C-9), 49.9 (C-17), 50.2 (25-OCH_3), 55.9 (7-OCH_3), 74.8 (C-25), 75.1 (C-7), 76.1 (C-3), 121.7 (C-6), 128.3 (C-

23), 136.7 (C-24), 146.2 (C-5), 206.7 (C-19); EI-MS (70 eV) *m/z* (rel. int.): 500 $[M]^+$ (8), 470 (20), 455 (22), 440 (40), 309 (13), 203 (33), 187 (31), 172 (97), 157 (47), 149 (52), 133 (49), 121 (60), 109 (100), 99 (72), 81 (37), 69 (34), 55 (60). (23*E*)-3*β*,7β,25-trihydroxycucbita-5,23-dien-19-al (CH93) Amorphous powder; IR (KBr)ν_{max} : 3425, 1715, 1660, 1470, 1380, 1000, 980 cm^{-1}; ^1H NMR (400 MHz, $CDCl_3$) : δ 0.72 (3H, s, H-30), 0.86 (3H, s, H-18), 0.88 (3H, d, *J* = 6.0 Hz, H-21), 1.03 (3H, s, H-29), 1.21 (3H, s, H-26), 1.22 (3H, s, H-27), 1.23 (3H, s, H-28), 3.55 (1H, br s, H-3), 3.95 (1H, br d, *J* = 5.2 Hz, H-7), 5.56 (2H, m, H-23, H-24), 5.87 (1H, d, *J* = 5.2 Hz, H-6), 9.70 (1H, br s, H-19); EI-MS (70 eV) *m/z* 454 $[M-H_2O]^+$ (2), 436 (6), 418 (43), 389 (100), 375 (8), 337 (10), 309 (17), 171 (29), 109 (31), 81 (16).

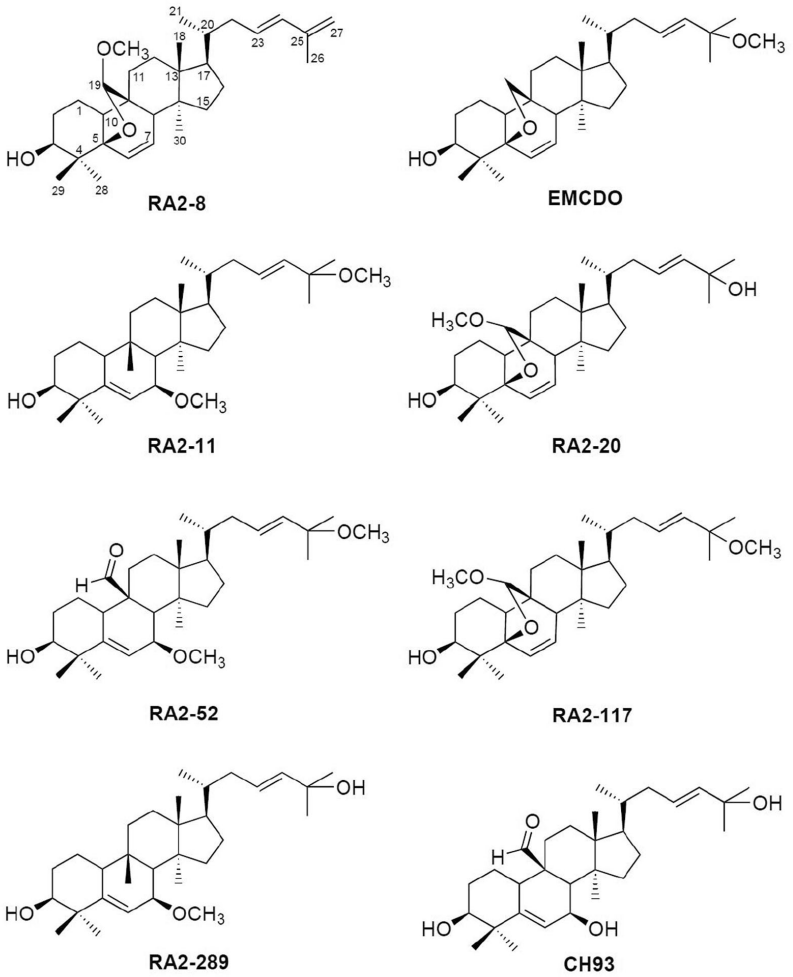

Figure 1. Chemical structures of eight compounds isolated from *M. charantia* fruit. The chemical structures of RA2-8, EMCDO, RA2-11, RA2-20, RA2-52, RA2-117, RA2-289, and CH93 are shown; their formal chemical names are stated in the text

3.2 Cytotoxicities of Compounds towards Two Hepatoma Cell Lines

To determine the non-toxic maximum working concentrations for cell-culture based assay, an MTT assay was utilized to evaluate the cytotoxicities of the isolated *Mormodica charantia* compounds and the anti-HBV positive control oltipraz (Chi et al., 1998). 2.2.15 (Doong, Tsai, Schinazi, Liotta, & Cheng, 1991) and PLC/PRF/5 (Marshall, Coulepis, Pringle, Dimitrakakis, & Gust, 1983) accumulate HBsAg and HBeAg after a longer period of culture; thus, the IC_{10} and IC_{50} of 9 days of treatment for 2.2.15 and 6 days for PLC/PRF/5 were determined. Table 1 illustrates the IC_{10} and IC_{50} concentrations of the tested compounds on two hepatoma cell lines. Based on these results, the working concentrations for further biological assays were: 5 μg/ml of EMCDO, RA2-11,oltipraz on both cell lines; 10 μg/ml of RA2-52 and RA2-117 on both cell lines; 10 μg/ml of RA2-8 on

2.2.15; 10 μg/ml of RA2-20, RA2-289 and CH93 on PLC/PRF/5; 7.5 μg/ml of RA2-8 on PLC/PRF/5; 7.5 μg/ml of RA2-289 and CH93 on 2.2.15; 5 μg/ml of RA2-20 on 2.2.15. Under our treatment conditions, more than 90% cells were viable.

Table 1. IC_{10} and IC_{50} of tested compounds on 2.2.15 and PLC/PRF/5 cell lines

			RA2-8	EMCDO	RA2-11	RA2-20	RA2-52	RA2-117	RA2-289	CH-93	oltipraz
2.2.15	day 3	IC_{10}	21.1 ± 2.1	20.4 ± 2.6	18.4 ± 0.8	12.2 ± 0.9	17.1 ± 1.3	16.8 ± 1.6	12.4 ± 1.0	13.7 ± 1.1	12.4 ± 1.3
		IC_{50}	23.5 ± 2.3	16.8 ± 2.2	21.3 ± 2.0	14.4 ± 1.4	23.8 ± 2.1	24.1 ± 2.3	17.8 ± 1.5	24.8 ± 2.3	18.5 ± 1.5
	day 6	IC_{10}	12.4 ± 1.2	7.8 ± 1.8	9.8 ± 0.3	10.1 ± 0.7	12.4 ± 1.1	13.8 ± 1.1	9.8 ± 0.7	10.1 ± 0.6	9.8 ± 0.7
		IC_{50}	21.4 ± 1.9	12.7 ± 1.3	18.6 ± 1.2	12.7 ± 1.1	19.6 ± 1.3	18.9 ± 1.4	13.1 ± 1.9	13.7 ± 1.2	13.9 ± 0.9
	day 9	IC_{10}	10.9 ± 0.8	5.1 ± 0.2	6.8 ± 0.4	6.4 ± 0.2	10.2 ± 0.9	10.1 ± 0.8	7.6 ± 0.3	7.8 ± 0.8	6.7 ± 0.2
		IC_{50}	19.4 ± 1.8	8.1 ± 0.3	14.2 ± 0.8	9.5 ± 0.7	16.1 ± 1.0	15.2 ± 1.2	10.8 ± 0.6	11.6 ± 1.0	10.2 ± 0.4
PLC/PRF/5	day 2	IC_{10}	14.1 ± 1.2	11.2 ± 1.0	11.9 ± 1.1	16.3 ± 0.9	20.4 ± 2.2	19.4 ± 1.9	14.3 ± 0.8	13.9 ± 0.7	11.1 ± 0.9
		IC_{50}	17.4 ± 1.6	14.8 ± 1.3	14.7 ± 1.2	18.7 ± 0.8	28.4 ± 2.4	21.1 ± 2.0	16.2 ± 1.0	18.7 ± 1.3	13.7 ± 1.1
	day 4	IC_{10}	11.5 ± 0.8	7.1 ± 0.5	8.9 ± 1.0	13.7 ± 0.7	14.5 ± 1.3	13.7 ± 1.3	12.3 ± 0.9	11.9 ± 1.0	8.4 ± 0.8
		IC_{50}	16.2 ± 0.9	8.4 ± 0.4	12.6 ± 1.1	14.9 ± 0.6	19.5 ± 1.2	15.4 ± 1.4	13.4 ± 0.7	14.4 ± 1.2	9.7 ± 0.4
	day 6	IC_{10}	8.7 ± 0.4	5.2 ± 0.3	6.8 ± 0.5	10.6 ± 0.3	11.1 ± 0.8	9.7 ± 0.6	9.8 ± 0.3	10.3 ± 0.6	5.4 ± 0.3
		IC_{50}	13.2 ± 0.6	7.6 ± 0.4	10.4 ± 0.6	13.2 ± 0.7	15.9 ± 1.0	12.1 ± 0.9	11.2 ± 0.7	12.3 ± 1.0	8.8 ± 0.9

3.3 Efficient Inhibition of HBs, HBe Antigen Production and Secreted HBV DNA by EMCDO

First of all, the suppression abilities of the compounds on HBs and HBe antigen production of cultured hepatoma cell lines were measured by ELISA assay. EMCDO revealed a dramatic inhibition effect after 3-9 days of treatment, which was comparable to the well-established HBV inhibitor oltipraz (Figures 2A and 2B). The significant HBsAg suppression activity of EMCDO exhibited an identical pattern on the PLC/PRF/5 cell line (Figure 2C). In addition to measuring the antigen production, the amount of HBV DNA in the culture medium was quantified. 2.2.15 cells were treated with various concentrations of EMCDO or oltipraz for 3 days. The EC_{50} of HBV DNA suppression was 4.58 μg/ml for oltipraz and 1.31 μg/ml for EMCDO; thus, EMCDO exhibited a better anti-HBV ability than oltipraz (Figure 2D).

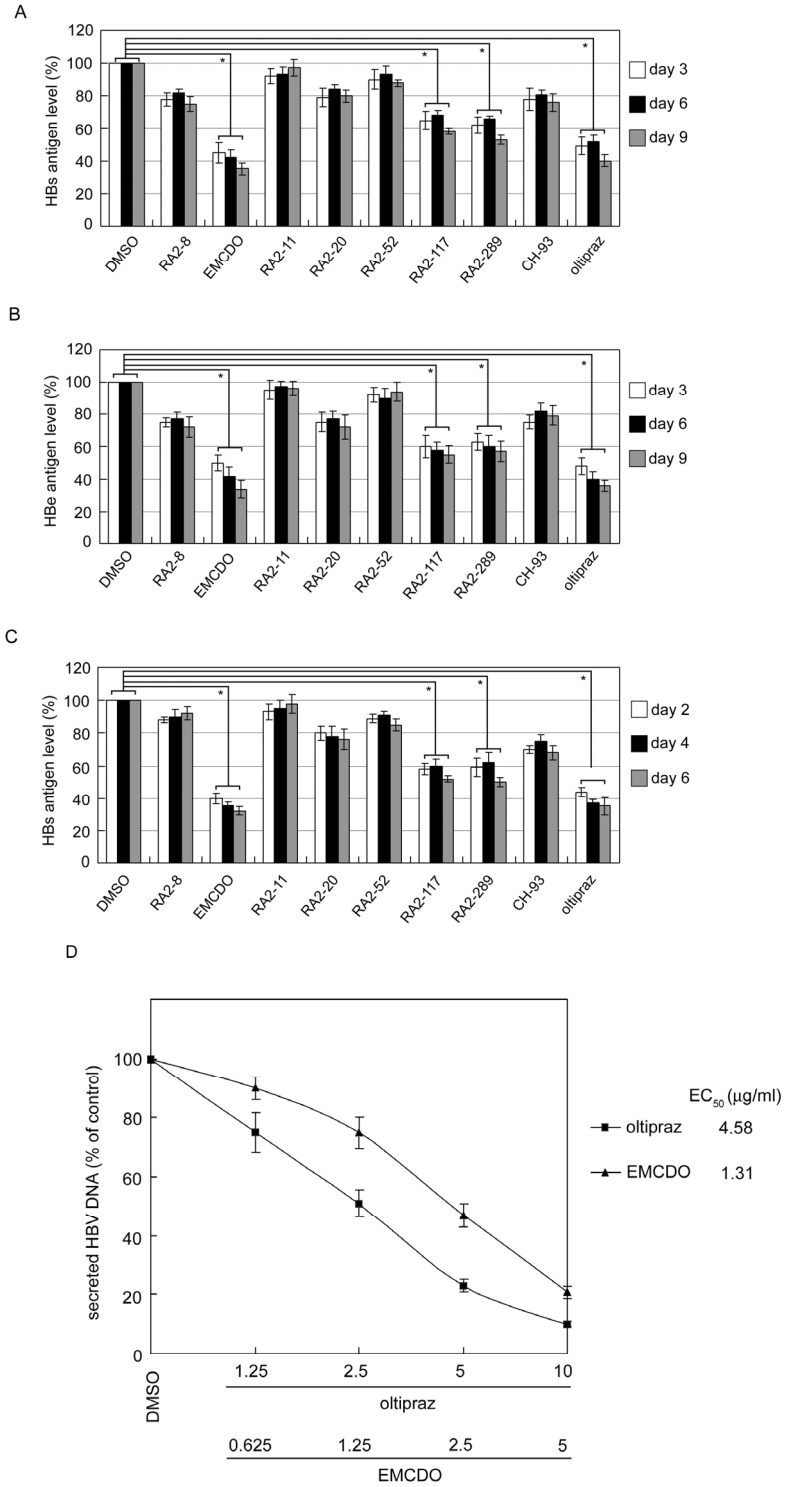

Figure 2. Reduction of HBV antigen and HBV DNA upon compound addition. 2.2.15 cells were treated with the indicated compounds for various time periods. Surface antigen (A) and e antigen HBe (B) levels were determined by ELISA and normalized against DMSO-treated cells. (C) PLC/PRF/5 cells were treated as indicated, and the surface antigen level was determined and normalized against DMSO-treated cells. Significant antigen inhibition is indicated by "*". (D) 2.2.15 cells were treated with EMCDO or oltipraz at various concentrations for 3 days, then the secreted HBV DNA was purified and subjected to semi-quantitative polymerase chain reaction. The EC50 concentration was calculated and is shown

3.4 p53 Involvement in EMCDO-Mediated Anti-HBV Effects

Oltipraz inhibits HBV *via* modulation of p53 (Chi et al., 1998). We then investigated whether EMCDO exerts its anti-HBV function through the activation of p53. The results clearly demonstrated the induction of p53 protein upon EMCDO and oltipraz treatment, and p53 expression showed more significant accumulation in cells treated with EMCDO (Figures 3A and 3B, panel 1). p53 phosphorylation at N-terminal serine residues is closely correlated with the transcriptional activation of its downstream genes (Jenkins, Durell, Mazur, & Appella, 2012). Our results showed greater serine phosphorylation induction and accumulation in EMCDO-treated cells than in oltipraz-treated cells (Figures 3A panels 2-5 and 3B panels 2-3). A p53-luc reporter was transfected into the cells, and activation of the synthetic promoter by the treatment will result in the stimulation of reporter expression. EMCDO and oltipraz induced luciferase activity in a dose-dependent manner, and the luciferase activity was fully inhibited in the cells co-transfected with dominant negative p53 (Figure 3C). Importantly, the p53 activation degree was greater in the EMCDO-treated cells than in the oltipraz-treated cells.

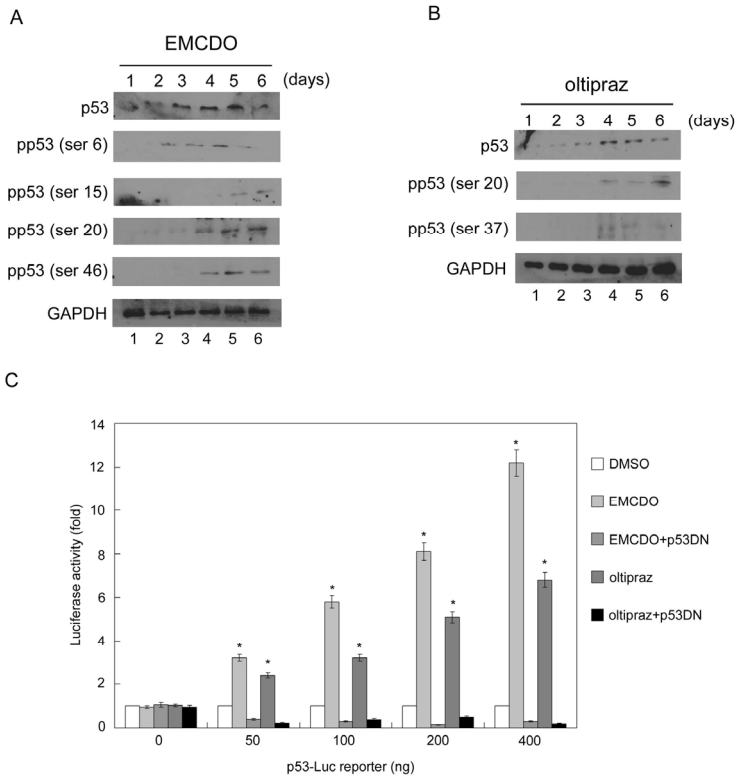

Figure 3. Activation of p53 by EMCDO. Western blotting analysis of (A) EMCDO- and (B) oltipraz-treated 2.2.15 cells. Total p53, phosphor-p53 and internal control GAPDH expression levels were determined by indicated antibodies. (C) Luciferase assay. 2.2.15 cells were treated with DMSO, EMCDO or oltipraz for 2 hrs, then transfected with p53-Luc reporter plasmid combined with pRKβGAL for 48hrs of incubation. p53DN plasmid was cotransfected into the indicated cells. The luciferase activation fold was calculated according to the transfection efficiency and normalized against time "0". Significant activation is indicated by "*"

3.5 Toxicity of EMCDO in Mice

In order to understand the possible application *in vivo*, we then evaluated the safety in a mouse model. Within 14 days observation, intraperitoneal injection of 500 mg/kg EMCDO did not produce any changes as compared with the control group. No mouse deaths suggested that EMCDO is not toxic at a dose of 500 mg/kg. Table 2 shows the mean body weight, organ weight and concentrations of liver and renal function markers. The liver function markers GOT and GPT, and renal function markers BUN and CRE, were all within the normal ranges. The body weight and organ weight of all mice at the end of experiment did not exhibit any significant changes.

Table 2. Biochemical analysis and organ weights of controls and EMCDO-treated mice

	Normal range	Control mice	EMCDO-treated mice
GOT (U/L)	59-247	159.5 ± 68.6	170.5 ± 32.5
GPT (U/L)	28-132	22.5 ± 9.8	26.2 ± 6.31
BUN (mg/dL)	18-29	22.8 ± 3.1	21.4 ± 1.62
CRE (mg/dL)	0.2-0.8	0.45 ± 0.06	0.49 ± 0.01
Heart (g)		0.126 ± 0.001	0.126 ± 0.001
Liver (g)		1.046 ± 0.002	0.965 ± 0.002
Spleen (g)		0.144 ± 0.001	0.161 ± 0.003
Lung (g)		0.160 ± 0.002	0.140 ± 0.004
Kidney (g)		0.301 ± 0.001	0.324 ± 0.002
Stomach (g)		0.264 ± 0.001	0.276 ± 0.003
Body weight (g)		24.5 ± 0.5	24.8 ± 0.4

3.6 Tumor Prevention Ability of EMCDO in a Nude Mouse Model

Subcutaneous inoculation of 2.2.15 cells induces tumor formation (Wu et al., 2011). EMCDO and oltipraz, as well as the negative control corn oil, were injected into nude mice *via* the peritoneal route. Compound injection was performed for 7 days, then 2.2.15 cells were inoculated. The observation period was 8 weeks, and compounds were injected once every 2 days within the 8-week period. At the end of the experiments, serum HBsAg, HBeAg and hepatoma marker AFP were dramatically reduced in EMCDO- and oltipraz-treated mice (Figure 4A). By monitoring the tumor size every 5 days after 2.2.15 inoculation, the average tumor size was observed to be much smaller in EMCDO- and oltipraz-treated mice (Figure 4B). Critically, the tumor suppression ability of EMCDO was a little better than that of oltipraz, especially during the later phase. The results clearly demonstrated the EMCDO is a good tumor prevention agent, the tumor suppression effect could be lasted for more longer time than oltipraz.

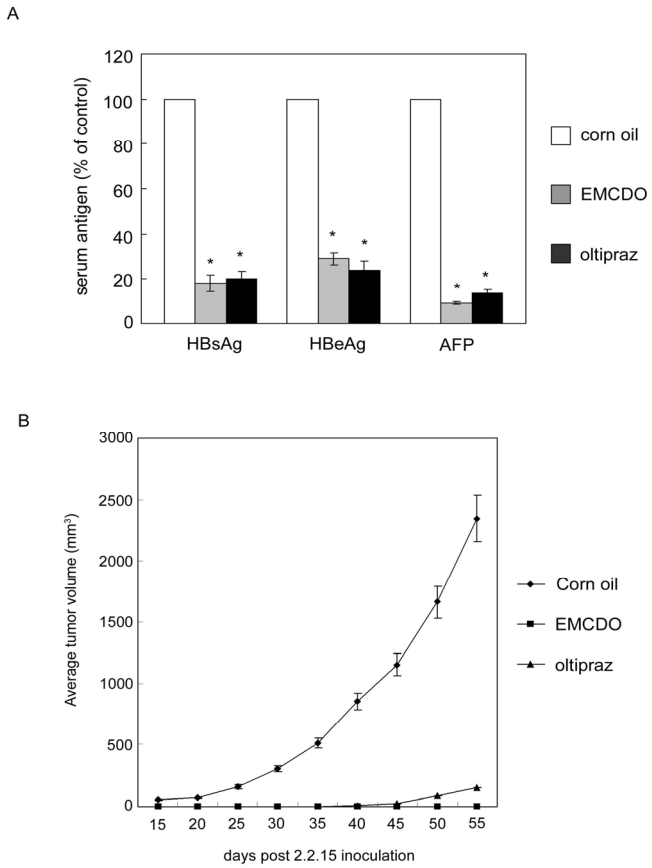

Figure 4. Tumor growth inhibition in a mouse model. (A) Serum was collected at the end of the experiment. The levels of HBV surface antigen, e antigen and AFP were determined by ELISA. Corn oil-treated mice served as the control. The antigen reduction percentages in EMCDO- or oltipraz-treated mice are shown in the y-axis. Significant reduction is indicated by "*". (B) Suppression of tumor volume of EMCDO- or oltipraz-injected mice. The x-axis indicates the days post-2.2.15 cells inoculation; the y-axis shows the average tumor volume of 6 mice

3.7 Inhibition of Inflammatory Mediators by EMCDO

Due to the close relationship between inflammation and cancer development, we studied further whether the anti-HBV effect of EMCDO is related to the anti-inflammation mechanism. LPS-treated RAW264.7 is a well-used model to evaluate the anti-inflammatory response (Kim, Hwang, & Han, 2013). The IC_{10} and IC_{50} cytotoxicities were determined in RAW264.7 cells upon EMCDO addition (Figure 5A); thus, the working concentration of the following experiments ensured the more than 90% of cells were viable. In a 24-hr experiment, we used a maximum EMCDO concentration of 5 μg/ml. The suppression dose effect of iNOS by curcumin was monitored (Figure 5B), and the effective concentration was correlated with a previous study (Cheung, Khor, & Kong, 2009). The LPS-stimulated expressions of inflammatory markers inducible nitric oxide synthase (iNOS) and cyclooxygenase-2 (COX-2) were repressed in the presence of EMCDO ranging from 1.25 to 5 μg/ml, and the repression efficiency was better than that of 7.5 μg/ml curcumin, a well-known efficient natural anti-inflammation polyphenol compound (Wang, Sun, Huang, & Zheng, 2013) (Figure 5C). LPS-treated RAW264.7 cells exhibited proinflammatory cytokines production and secretion, including TNF-α, IL-6 and IL-1β (Qi et al., 2012). As expected, the three proinflammatory cytokines were dramatically repressed in the presence of EMCDO in a dose-dependent manner. At a non-cytotoxic concentration of 5 μg/ml EMCDO, the cytokine repression ability was comparable to that of the well-known anti-inflammation compound curcumin (Figure 5D).

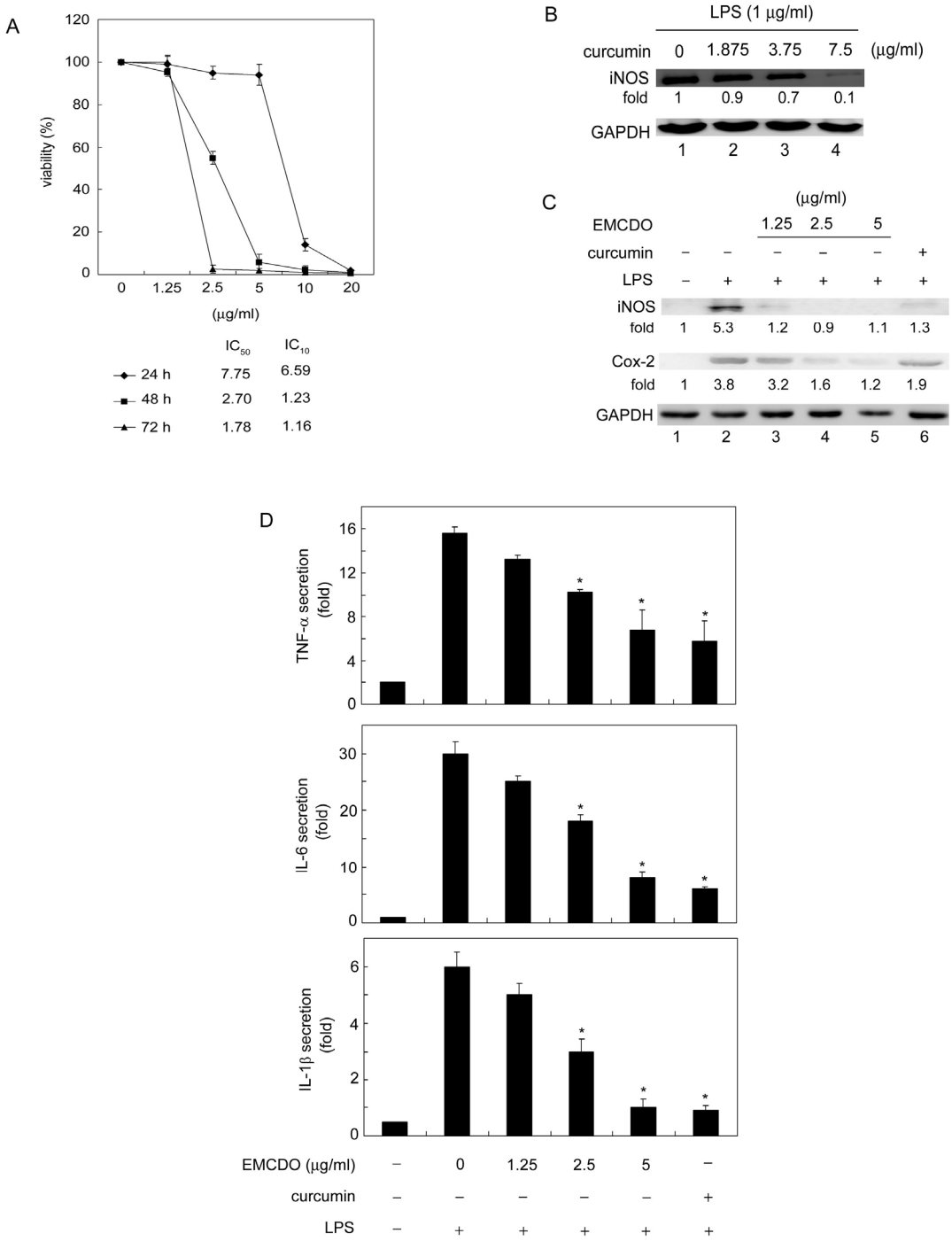

Figure 5. Anti-inflammation ability of EMCDO. (A) Trypan blue exclusion assay. RAW264.7 cells were incubated with various concentrations of EMCDO for 24, 48 and 72 hrs. The viable and dead cells were differentiated by trypan blue dye. The y-axis shows the viable cell percentage normalized against non-treated cells; the IC_{50} and IC_{10} are indicated. (B) Curcumin inhibits LPS-induced iNOS expression. Western blotting analysis of RAW264.7 cells treated with LPS and curcumin for 24 hrs of incubation. 50 μg soluble protein were subjected to SDS-PAGE. The iNOS expression fold was normalized against GAPDH and compared with lane 1. (C) EMCDO suppressed iNOS and COX-2 expression dose-dependently. Western blotting analysis of RAW264.7 cells treated as indicated. The expression level was normalized against GAPDH and compared with lane 1. (D) Measurement of proinflammatory cytokines by ELISA. The y-axis shows the cytokine secretion fold normalized against conditioned media of non-treated RAW264.7 cells. The x-axis indicates the compound treatment of cells

3.8 Activation of NF-κB, Not MAPK Signaling, by EMDCO

Previous studies have indicated that MAPK signaling and NF-κB play roles in mediating anti-inflammation in some cell culture-based systems, including RAW264.7 cells (Yuan, Chen, Sun, Guan, & Xu, 2013). In these assay systems, LPS increases IκBα and MAPKs phosphorylation (Yoon et al., 2010; Meng, Yan, Deng, Gao, & Niu, 2013). To investigate the host cell signaling participation in mediating the EMCDO effects, the phosphorylation levels of JNK, p38, ERK and IκBα were examined by specific phospho-antibodies. The results clearly showed that phosphorylation of JNK, p38 and ERK was not altered upon EMCDO or curcumin treatment (Figure 6A, panel 1-3), while the increased phosphorylation of IκBα by LPS was reduced by 5 μg/ml EMCDO and curcumin (Figure 6A, panel 4). To further confirm the involvement of NF-κB, a luciferase reporter plasmid containing an upstream NF-κB responsive element was transfected into compound-treated cells. Figure 6B illustrates that the up-regulated luciferase activity by LPS was reduced by EMCDO in a concentration-dependent pattern, comparable to the positive control curcumin. Thus, the current findings suggested that NF-κB-related signaling may have a critical regulation in EMCDO's anti-HBV and anti-inflammation effects.

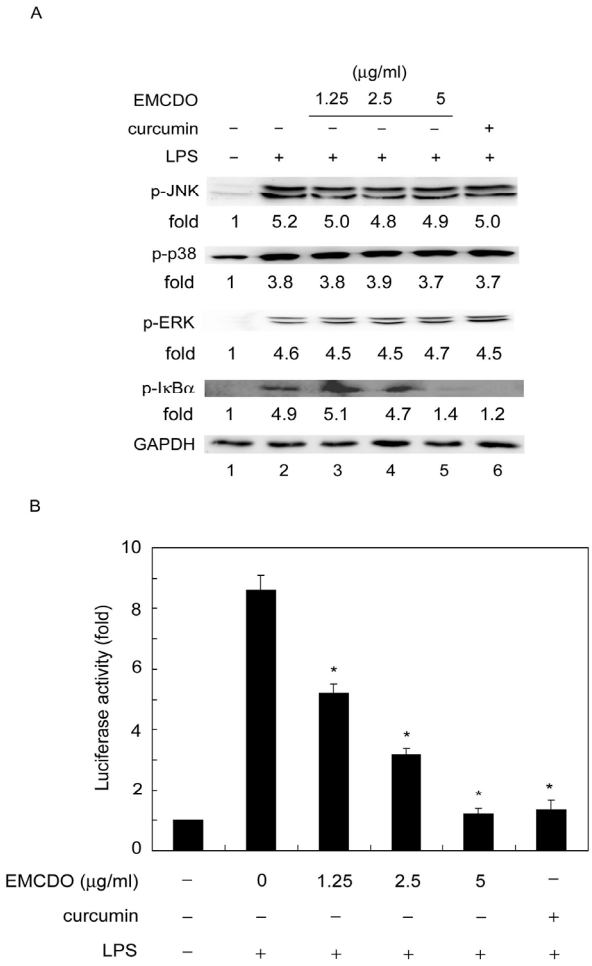

Figure 6. (A) Western blotting analysis. RAW264.7 cells were pre-treated with the indicated compound for 2 hrs, then LPS was added for a further 6 hrs of incubation. Soluble cell lysates were harvested and subjected to SDS-PAGE. The phosphor-protein expression level and internal control GAPDH are shown. The fold induction was determined using software and compared with lane 1. (B) Luciferase assay. Compounds were pre-treated for 2 hrs then co-transfected with NF-κB-Luc and pRKβGAL. After 24 hrs, LPS was added and incubated for an additional 24 hrs. Luciferase and β-galatosidase activities were measured. The data are expressed as the luciferase activation fold by normalization of the transfection efficiency and compared with non-treated control cells. Significant suppression is indicated by "*"

3.9 Anti-Inflammation Ability of EMCDO in vivo

In the case of the ear edema mouse model, EMCDO effectively inhibited the ear thickness in a dose-dependent manner by topical application. Comparison of indomethacin and EMCDO using the same concentration of 1.25 μg/20 μl showed that the edema inhibition ability of EMCDO is better than that of the classic non-steroidal anti-inflammatory drug indomethacin after 6 and 16 hrs of treatment. Importantly, the anti-inflammation efficiency of EMCDO was still significant at 1.25 μg/20 μl after 24 hrs of application. At a lower concentration of EMCDO, the anti-inflammation effect was apparent after 6 hrs of application (Figure 7). Taken together, these results showed that EMCDO is a low-toxicity, highly-effective anti-inflammation compound. The inflammation-relaxing ability of EMCDO is rapid and more potent than that of indomethacin.

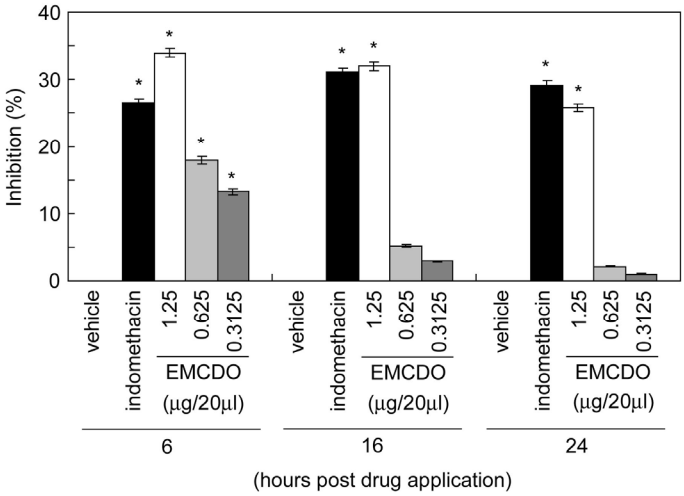

Figure 7. Inhibition of ear edema by EMCDO. Ear thickness was measured before and after TPA application at 30 min. Then, indomethacin and various concentrations of EMCDO were topically applied for different time periods. The y-axis represents the ear thickness reduction percentage. Significant inhibition of ear thickening is indicated by "*"

4. Discussion

The current investigation demonstrated that one *Mormodica charantia* compound, EMCDO, isolated in our laboratory possessed good anti-HBV, anti-tumor and anti-acute inflammation activities. Based upon the HBV-secreting cell line, a mouse macrophage model and *in vivo* assays, it was confirmed that EMCDO is a low-toxicity compound of high biological efficacy.

All the isolated compounds, except for RA2-11 and RA2-52, showed anti-HBV activity. Comparing their structures, the cucurbitane-type triterpenes with a 5β,19-epoxy moiety in the skeleton, RA2-8, EMCDO, RA2-20, and RA2-117, always exhibited a significant anti-HBV effect. In particular, EMCDO without the methoxy substituent at C-19 showed the greatest level of anti-HBV activity. Additionally, RA2-289 possesses a hydroxy group at C-25 in the side chain, and exhibited a higher anti-HBV activity than its methyl ether derivative, RA2-11. Furthermore, the simultaneous methylation at C-7 and C-25 decreased the activity level as compared with the activity results of CH-93 and RA2-52. Thus, for the cucurbitane-type triterpenes, a 5β,19-epoxy moiety in the skeleton, along with the hydroxy free form at C-7 and C-25 in the side chain, may be important for their anti-HBV activity expression.

The underlying molecular mechanisms participating in hepatocellular carcinoma development remain incompletely understood. It is well-known that intrinsic and extrinsic inflammatory signaling pathways converge and cooperate in amplifying the cancer risk and driving cancer cell formation. However, the cancer-associated inflammation response is often persistent and chronic, inducing uncontrolled pathological signals in the tumor microenvironment; thus, cellular proliferation, migration, invasion and angiogenesis will occur (Wai & Kuo, 2012).

HBV and HCV infections result in liver inflammation and further liver cancer development. During acute

infection, viral antigens activate immune cells and could induce the infected cells undergoing apoptosis. The result of cell death caused cell regeneration (Bertoletti, Maini, & Ferrari, 2010). Furthermore, current evidence indicates that chronic inflammation will lead to gene mutation and genome instability, and the accumulated mutated gene plays critical roles in liver carcinogenesis (Brechot et al., 2010). For example, HBV X protein and HCV core protein are expressed during infection, and these viral oncoproteins interact with the cellular homeostasis machinery, affect cellular gene expression and regulation, and also participate in liver inflammation (Ray, Steele, Meyer, & Ray, 1997).

Various cellular pathways are activated during a prolonged inflammation process in the liver, such as NF-κB (Assenat, Grebal-Chaloin, Maurel, Vilarem, & Pascussi, 2006) and JAK/STAT3 (Park et al., 2010), as well as MAPK signalings (Ma, Ding, Zhang, & Liu, 2014). EMCDO alleviated the inflammation mediator production and ear inflammation, possibly through the activation of NF-κB in the RAW264.7 system, but no effects on MAPK were observed. Previous studies have indicated a dual function of NF-κB in hepatocarcinogenesis: NF-κB can activate cell-protecting gene expression and then prevent excess cell death, thus limiting the subsequent cell transformation (Luedde et al., 2007). On the other hand, NF-κB may constitute a link between inflammation and cancer (Pikarsky et al., 2004). Additionally, the inflammation response also regulates epigenetic change, including DNA methylation, histone modifications, as well as non-coding RNAs in hepatocytes (Martin & Herceg, 2012).

One important component of the immune system to cope with foreign antigens is cytokines. The liver contains many various cell types that are susceptible to the influences of cytokines. Hepatocytes bear cytokine receptors, such as IL-6, IL-1 and TNF-α. The cytokines released from Th1 cells normally function as proinflammatory cytokines; on the other hand, Th2 cytokines, such as IL-4, IL-8, IL-10, and IL-5, induce anti-inflammatory responses. In fact, many cytokines have pleiotrophic activities, which could function in synergistic or antagonistic manner. Due to the enriched immune cells located in liver, the evidence had been indicated these inflammatory cells secreted cytokines and further cause liver injury characteristic of acute HBV (Rehermann, 2003). In addition, hepatic viruses are able to evade the immune system and persist *via* a variety of mechanisms, the major way being to rapidly mutate under immune pressure. Recently, several studies have described that changes in Th1 and Th2 cytokines expression result from various treatment regimens which correlated in HCC metastasis or recurrence in patients (Budhu & Wang, 2006).

Malignant neoplasia is the result of multiple genetic defects successively accumulating over a period of time in genes mainly controlling proliferation, differentiation and cell death (Stephenson, Abouassaly, & Klein, 2010), yet most current anticancer therapies involve mainly or only the modulation of a single target. As a result, research concentrating on the discovery of multi-target new agents and new treatment strategies is therefore of vital importance (Guruswamy & Rao, 2008). Broadly defined, cancer chemoprevention applies to the inhibition or reversal of oncogenesis, at a variety of time points, to suppress the occurrence of *in situ* or invasive cancers using natural, synthetic, biologic or chemical agents (Desai et al., 2008). Although the principle of chemoprevention has been clearly demonstrated in both animal and clinical trials, none of the existing chemopreventive agents is ideal, because of either a lack of efficacy or toxic side effects (Lam, Macaulay, Leriche, & Gazdar, 2003). Accumulation of *in vitro* evidence demonstrating the inhibitory effects of certain natural products on liver cancer cells (Fang, Hsu, Lin, & Yen, 2010). The anti-carcinogenic activity of cucurbitane-type triterpenoids has been clearly demonstrated in two-stage carcinogenesis testing in skin tumors (Takasaki et al., 2003). The triterpenoid saponin-rich G. oldhamiana root extract (TGOE) selectively inhibited the proliferation of hepatoma SMMC-7721 cells in a dose-dependent manner, while the cytotoxic effects of TGOE on normal hepatocyte L02 cells were much lower. TGOE preferentially induced apoptosis in SMMC-7721 cells due to the regulation of caspase-3 and mitogen-activated protein kinases (MAPKs) (Zhang, Luo, Zhang, & Kong, 2013). In conclusion, the chemical structure determination of 8 isolated *Mormodica charantia* compounds. EMCDO significantly reduced HBV antigens and DNA secretion in hepatoma cell lines, prevented the tumor formation induced by a HBV-producing cell line in nude mice model. In addition, EMCDO downregulated inflammatory mediators in LPS-treated RAW264.7 cells and inhibited edema in the TPA-treated mouse ear. Our data suggested that EMCDO may have potential beneficial effects against HBV and inflammation response, subsequently preventing hepatocellular carcinoma development. To prove the clinical uses of EMCDO, efforts to elucidate the underlying mechanism and more animal tests are needed.

References

Abe, A., Inoue, K., Tanaka, T., Kato, J., Kajiyama, N., Kawaguchi, R., … Kohara, M. (1999). Quantitation of hepatitis B virus genomic DNA by real-time detection PCR. *J Clin Microbiol, 37*(9), 2899-2903.

Acs, G., Sells, M. A., Purcell, R. H., Price, P., Engle, R., Shapiro, M., & Popper, H. (1987). Hepatitis B virus produced by transfected Hep G2 cells causes hepatitis in chimpanzees. *Proc Natl Acad Sci USA,* 84(13), 4641-4644. http://dx.doi.org/10.1073/pnas.84.13.4641

Akihisa, T., Hayakawa, Y., Tokuda, H., Banno, N., Shimizu, N., Suzuki, T., & Kimura, Y. (2007). Cucurbitane glycosides from the fruits of Siraitia gros venorii and their inhibitory effects on Epstein-Barr virus activation. *J Nat Prod, 70*(5), 783-788. http://dx.doi.org/10.1021/np068074x

Alexander, B., Browse, D. J., Reading, S. J., & Benjamin, I. S. (1999). A simple and accurate mathematical method for calculation of the EC50. *J Pharmacol Toxicol Methods, 41*(2-3), 55-58. http://dx.doi.org/10.1016/S1056-8719(98)00038-0

Aslam, M. N., Bergin, I., Naik, M., Hampton, A., Allen, R., Kunkel, S. L., … Varani, J. (2012). A multi-mineral natural product inhibits liver tumor formation in C57BL/6 mice. *Biol Trace Elem Res, 147*(1-3), 267-274. http://dx.doi.org/10.1007/s12011-011-9316-2

Assenat, E., Gerbal-chaloin, S., Maurel, P., Vilarem, M. J., & Pascussi, J. M. (2006). Is nuclear factor kappa-B the missing link between inflammation, cancer and alteration in hepatic drug metabolism in patients with cancer? *Eur J Cancer, 42*(6), 785-792. http://dx.doi.org/10.1016/j.ejca.2006.01.005

Berasain, C., Castillo, J., Perugorria, M. J., Latasa, M. U., Prieto, J., & Avila, M. A. (2009a). Inflammation and liver cancer: new molecular links. *Ann N Y Acad Sci, 1155*, 206-221. http://dx.doi.org/10.1111/j.1749-6632.2009.03704.x

Berasain, C., Perugorria, M. J., Latasa, M. U., Castillo, J., Goni, S., Santamaria, M., … Avila, M. A. (2009b). The epidermal growth factor receptor: a link between inflammation and liver cancer. *Exp Biol Med (Maywood), 234*(7), 713-725. http://dx.doi.org/10.3181/0901-MR-12

Bertoletti, A., Maini, M. K., & Ferrari, C. (2010). The host-pathogen interaction during HBV infection: immunological controversies. *Antivir Ther, 15*(Suppl. 3), 15-24. http://dx.doi.org/10.3851/IMP1620

Brechot, C., Kremsdorf, D., Soussan, P., Pineau, P., Dejean, A., Paterlini-Brechot, P., & Tiollais, P. (2010). Hepatitis B virus (HBV)-related hepatocellular carcinoma (HCC): molecular mechanisms and novel paradigms. *Pathol Biol (Paris), 58*(4), 278-287. http://dx.doi.org/10.1016/j.patbio.2010.05.001

Budhu, A., & Wang, X. W. (2006). The role of cytokines in hepatocellular carcinoma. *J Leukoc Biol, 80*(6), 1197-1213. http://dx.doi.org/10.1189/jlb.0506297

Cetin, Y., & Bullerman, L. B. (2005). Cytotoxicity of Fusarium mycotoxins to mammalian cell cultures as determined by the MTT bioassay. *Food Chem Toxicol, 43*(5), 755-764. http://dx.doi.org/10.1016/j.fct.2005.01.016

Chang, C. D., Lin, P. Y., Liao, M. H., Chang, C. I., Hsu, J. L., Yu, F. L., … Shih, W. L. (2013). Suppression of apoptosis by pseudorabies virus Us3 protein kinase through the activation of PI3-K/Akt and NF-kappaB pathways. *Res Vet Sci, 95*(2), 764-774. http://dx.doi.org/10.1016/j.rvsc.2013.06.003

Chang, C. I., Chen, C. R., Liao, Y. W., Cheng, H. L., Chen, Y. C., & Chou, C. H. (2008). Cucurbitane-type triterpenoids from the stems of momordica charantia. *J Nat Prod, 71*(8), 1327-1330. http://dx.doi.org/10.1021/np070532u

Chemin, I. (2010). Evaluation of a hepatitis B vaccination program in Taiwan: impact on hepatocellular carcinoma development. *Future Oncol, 6*(1), 21-23. http://dx.doi.org/10.2217/fon.09.158

Chen, J. C., Zhang, G. H., Zhang, Z. Q., Qiu, M. H., Zheng, Y. T., Yang, L. M., & Yu, K. B. (2008). Octanorcucurbitane and cucurbitane triterpenoids from the tubers of Hemsleya endecaphylla with HIV-1 inhibitory activity. *J Nat Prod, 71*(1), 153-155. http://dx.doi.org/10.1021/np0704396

Cheung, K. L., Khor, T. O., & Kong, A. N. (2009). Synergistic effect of combination of phenethyl isothiocyanate and sulforaphane or curcumin and sulforaphane in the inhibition of inflammation. *Pharm Res, 26*(1), 224-231. http://dx.doi.org/10.1007/s11095-008-9734-9

Chi, W. J., Doong, S. L., Lin-Shiau, S. Y., Boone, C. W., Kelloff, G. J., & Lin, J. K. (1998). Oltipraz, a novel inhibitor of hepatitis B virus transcription through elevation of p53 protein. *Carcinogenesis, 19*(12), 2133-2138. http://dx.doi.org/10.1093/carcin/19.12.2133

Desai, A. G., Qazi, G. N., Ganju, R. K., El-Tamer, M., Singh, J., Saxena, A. K., … Bhat, H. K. (2008). Medicinal plants and cancer chemoprevention. *Curr Drug Metab, 9*(7), 581-591. http://dx.doi.org/10.2174/138920008785821657

Doong, S. L., Tsai, C. H., Schinazi, R. F., Liotta, D. C., & Cheng, Y. C. (1991). Inhibition of the replication of hepatitis B virus in vitro by 2',3'-dideoxy-3'-thiacytidine and related analogues. *Proc Natl Acad Sci USA, 88*(19), 8495-8499. http://dx.doi.org/10.1073/pnas.88.19.8495

Elgouhari, H. M., Abu-Rajab Tamimi, T. I., & Carey, W. D. (2008). Hepatitis B virus infection: understanding its epidemiology, course, and diagnosis. *Cleve Clin J Med, 75*(12), 881-889. http://dx.doi.org/10.3949/ccjm.75a.07019

Fang, S. C., Hsu, C. L., Lin, H. T., & Yen, G. C. (2010). Anticancer effects of flavonoid derivatives isolated from Millettia reticulata Benth in SK-Hep-1 human hepatocellular carcinoma cells. *J Agric Food Chem, 58*(2), 814-820. http://dx.doi.org/10.1021/jf903216r

Guruswamy, S., & Rao, C. V. (2008). Multi-Target Approaches in Colon Cancer Chemoprevention Based on Systems Biology of Tumor Cell-Signaling. *Gene Regul Syst Bio, 2*, 163-176.

Jenkins, L. M., Durell, S. R., Mazur, S. J., & Appella, E. (2012). p53 N-terminal phosphorylation: a defining layer of complex regulation. *Carcinogenesis, 33*(8), 1441-1449. http://dx.doi.org/10.1093/carcin/bgs145

Kim, S. Y., Hwang, J. S., & Han, I. O. (2013). Tunicamycin inhibits Toll-like receptor-activated inflammation in RAW264.7 cells by suppression of NF-kappaB and c-Jun activity via a mechanism that is independent of ER-stress and N-glycosylation. *Eur J Pharmacol, 721*(1-3), 294-300. http://dx.doi.org/10.1016/j.ejphar

Lam, S., MacAulay, C., LeRiche, J. C., & Gazdar, A. F. (2003). Key issues in lung cancer chemoprevention trials of new agents. *Recent Results Cancer Res, 163*, 182-195; Discussion, 264-186. http://dx.doi.org/10.1007/978-3-642-55647-0_17

Liao, Y. W., Chen, C. R., Kuo, Y. H., Hsu, J. L., Shih, W. L., Cheng, H. L., … Chang, C. I. (2012). Cucurbitane-type triterpenoids from the fruit pulp of Momordica charantia. *Nat Prod Commun, 7*(12), 1575-1578.

Luedde, T., Beraza, N., Kotsikoris, V., van Loo, G., Nenci, A., De Vos, R., … Pasparakis, M. (2007). Deletion of NEMO/IKKgamma in liver parenchymal cells causes steatohepatitis and hepatocellular carcinoma. *Cancer Cell, 11*(2), 119-132. http://dx.doi.org/10.1016/j.ccr.2006.12.016

Ma, J. Q., Ding, J., Zhang, L., & Liu, C. M. (2014). Ursolic acid protects mouse liver against CCl-induced oxidative stress and inflammation by the MAPK/NF-kappaB pathway. *Environ Toxicol Pharmacol, 37*(3), 975-983. http://dx.doi.org/10.1016/j.etap.2014.03.011

Maddrey, W. C. (2000). Hepatitis B: an important public health issue. *J Med Virol, 61*(3), 362-366. http://dx.doi.org/10.1002/1096-9071(200007)61:3<362::AID-JMV14>3.0.CO;2-I

Marshall, J., Coulepis, A., Pringle, R., Dimitrakakis, M., & Gust, I. D. (1983). The effect of glucocorticoid hormones on release of HBsAg from PLC/PRF/5 (Alexander) hepatoma cells. *Acta Virol, 27*(5), 429-433.

Martin, M., & Herceg, Z. (2012). From hepatitis to hepatocellular carcinoma: a proposed model for cross-talk between inflammation and epigenetic mechanisms. *Genome Med, 4*(1), 8. http://dx.doi.org/10.1186/gm307

Marusawa, H., & Jenkins, B. J. (2014). Inflammation and gastrointestinal cancer: An overview. *Cancer Lett, 345*(2), 153-156. http://dx.doi.org/10.1016/j.canlet.2013.08.025

Meng, Z., Yan, C., Deng, Q., Gao, D. F., & Niu, X. L. (2013). Curcumin inhibits LPS-induced inflammation in rat vascular smooth muscle cells in vitro via ROS-relative TLR4-MAPK/NF-kappaB pathways. *Acta Pharmacol Sin, 34*(7), 901-911. http://dx.doi.org/10.1038/aps.2013.24

Netea, M. G., Drenth, J. P., De Bont, N., Hijmans, A., Keuter, M., Dharmana, E., … van der Meer, J. W. (1996). A semi-quantitative reverse transcriptase polymerase chain reaction method for measurement of MRNA for TNF-alpha and IL-1 beta in whole blood cultures: its application in typhoid fever and exentric exercise. *Cytokine, 8*(9), 739-744. http://dx.doi.org/10.1006/cyto.1996.0098

Park, E. J., Lee, J. H., Yu, G. Y., He, G., Ali, S. R., Holzer, R. G., … Karin, M. (2010). Dietary and genetic obesity promote liver inflammation and tumorigenesis by enhancing IL-6 and TNF expression. *Cell, 140*(2), 197-208. http://dx.doi.org/10.1016/j.cell.2009.12.052

Pikarsky, E., Porat, R. M., Stein, I., Abramovitch, R., Amit, S., Kasem, S., … Ben-Neriah, Y. (2004). NF-kappaB functions as a tumour promoter in inflammation-associated cancer. *Nature, 431*(7007), 461-466. http://dx.doi.org/10.1038/nature02924

Qi, S., Xin, Y., Guo, Y., Diao, Y., Kou, X., Luo, L., & Yin, Z. (2012). Ampelopsin reduces endotoxic inflammation via repressing ROS-mediated activation of PI3K/Akt/NF-kappaB signaling pathways. *Int Immunopharmacol, 12*(1), 278-287. http://dx.doi.org/10.1016/j.intimp.2011.12.001

Ray, R. B., Steele, R., Meyer, K., & Ray, R. (1997). Transcriptional repression of p53 promoter by hepatitis C virus core protein. *J Biol Chem, 272*(17), 10983-10986. http://dx.doi.org/10.1074/jbc.272.17.10983

Rehermann, B. (2003). Immune responses in hepatitis B virus infection. *Semin Liver Dis, 23*(1), 21-38. http://dx.doi.org/10.1055/s-2003-37586

Shih, W. L., Kuo, M. L., Chuang, S. E., Cheng, A. L., & Doong, S. L. (2000). Hepatitis B virus X protein inhibits transforming growth factor-beta -induced apoptosis through the activation of phosphatidylinositol 3-kinase pathway. *J Biol Chem, 275*(33), 25858-25864. http://dx.doi.org/10.1074/jbc.M003578200

Shih, W. L., Yu, F. L., Chang, C. D., Liao, M. H., Wu, H. Y., & Lin, P. Y. (2013). Suppression of AMF/PGI-mediated tumorigenic activities by ursolic acid in cultured hepatoma cells and in a mouse model. *Mol Carcinog, 52*(10), 800-812. http://dx.doi.org/10.1002/mc.21919

Stephenson, A. J., Abouassaly, R., & Klein, E. A. (2010). Chemoprevention of prostate cancer. *Urol Clin North Am, 37*(1), 11-21. Table of Contents. http://dx.doi.org/10.1016/j.ucl.2009.11.003

Stockert, J. C., Blazquez-Castro, A., Canete, M., Horobin, R. W., & Villanueva, A. (2012). MTT assay for cell viability: Intracellular localization of the formazan product is in lipid droplets. *Acta Histochem, 114*(8), 785-796. http://dx.doi.org/10.1016/j.acthis.2012.01.006

Takasaki, M., Konoshima, T., Murata, Y., Sugiura, M., Nishino, H., Tokuda, H., … Yamasaki, K. (2003). Anticarcinogenic activity of natural sweeteners, cucurbitane glycosides, from Momordica grosvenori. *Cancer Lett, 198*(1), 37-42. http://dx.doi.org/10.1016/S0304-3835(03)00285-4

Vasconcelos, J. F., Teixeira, M. M., Barbosa-Filho, J. M., Lucio, A. S., Almeida, J. R., de Queiroz, L. P., … Soares, M. B. (2008). The triterpenoid lupeol attenuates allergic airway inflammation in a murine model. *Int Immunopharmacol, 8*(9), 1216-1221. http://dx.doi.org/10.1016/j.intimp.2008.04.011

Wai, P. Y., & Kuo, P. C. (2012). Intersecting pathways in inflammation and cancer: Hepatocellular carcinoma as a paradigm. *World J Clin Oncol, 3*(2), 15-23. http://dx.doi.org/10.5306/wjco.v3.i2.15

Wang, H., Syrovets, T., Kess, D., Buchele, B., Hainzl, H., Lunov, O., … Simmet, T. (2009). Targeting NF-kappa B with a natural triterpenoid alleviates skin inflammation in a mouse model of psoriasis. *J Immunol, 183*(7), 4755-4763. http://dx.doi.org/10.4049/jimmunol.0900521

Wang, L. L., Sun, Y., Huang, K., & Zheng, L. (2013). Curcumin, a potential therapeutic candidate for retinal diseases. *Mol Nutr Food Res, 57*(9), 1557-1568. http://dx.doi.org/10.1002/mnfr.201200718

Wu, H. Y., Chang, C. I., Lin, B. W., Yu, F. L., Lin, P. Y., Hsu, J. L., … Shih, W. L. (2011). Suppression of hepatitis B virus x protein-mediated tumorigenic effects by ursolic Acid. *J Agric Food Chem, 59*(5), 1713-1722. http://dx.doi.org/10.1021/jf1045624

Yoon, W. J., Moon, J. Y., Kang, J. Y., Kim, G. O., Lee, N. H., & Hyun, C. G. (2010). Neolitsea sericea essential oil attenuates LPS-induced inflammation in RAW 264.7 macrophages by suppressing NF-kappaB and MAPK activation. *Nat Prod Commun, 5*(8), 1311-1316.

Yuan, F., Chen, J., Sun, P. P., Guan, S., & Xu, J. (2013). Wedelolactone inhibits LPS-induced pro-inflammation via NF-kappaB pathway in RAW 264.7 cells. *J Biomed Sci, 20*, 84. http://dx.doi.org/10.1186/1423-0127-20-84

Zhang, W., Luo, J. G., Zhang, C., & Kong, L. Y. (2013). Different apoptotic effects of triterpenoid saponin-rich Gypsophila oldhamiana root extract on human hepatoma SMMC-7721 and normal human hepatic L02 cells. *Biol Pharm Bull, 36*(7), 1080-1087. http://dx.doi.org/10.1248/bpb.b12-01069